

Structural Investigation of Homonuclear Pt₂ and Heteronuclear PdPt Complexes Containing a Metal–Metal Bond Bridged by Hydrido and Sulfido Ligands

WILLIAM CLEGG,^{a*} MERCÈ CAPDEVILA,^b PILAR GONZÁLEZ-DUARTE^b AND JOAN SOLA^b

^aDepartment of Chemistry, University of Newcastle, Newcastle upon Tyne NE1 7RU, England, and ^bDepartament de Química, Universitat Autònoma de Barcelona, 08193 Bellaterra, Barcelona, Spain. E-mail: w.clegg@ncl.ac.uk

(Received 2 December 1994; accepted 28 July 1995)

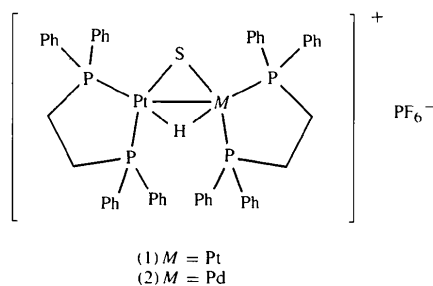
Abstract

The complex [Pt₂(μ-H)(μ-S)(dppe)₂](PF₆) undergoes a displacive order–disorder transformation at ca 230 K. The low-temperature structure is ordered with one cation–anion pair as the asymmetric unit in space group *P*2₁/*n*. At room temperature the *b* axis is halved and the space group is *P*2/*n*, imposing crystallographic twofold rotation symmetry on both ions; the anion shows major disorder and there is probably minor disorder in the cation, but its internal geometry remains essentially unchanged. The heteronuclear complex [PdPt(μ-H)(μ-S)(dppe)₂](PF₆) is isostructural with the Pt₂ complex at room temperature. All three structures have been determined crystallographically and both complexes have been extensively characterized by NMR spectroscopy, unambiguously confirming the genuine heteronuclear nature of the mixed-metal complex and the presence of the bridging hydride ligand.

1. Introduction

As part of a wide-ranging programme of research in the coordination chemistry of aminoalkanethiolates (aliphatic mercaptoamines), we have prepared and structurally characterized palladium(II) and platinum(II) complexes of various aminoalkanethiolato ligands (Capdevila, Clegg, González-Duarte & Mira, 1992; Capdevila, Clegg, González-Duarte, Harris, Mira, Sola & Taylor, 1992; Capdevila, González-Duarte, Foces-Foces, Hernández Cano & Martínez-Ripoll, 1990; Capdevila, Clegg, González-Duarte, Jarid & Lledós, 1996). Reaction of the two mononuclear platinum complexes [Pt(SC₅H₉NMe)₂(dppe)] and [PtCl₂(dppe)] in organic solvents gives the dinuclear cationic species [Pt₂(μ-SC₅H₉NMe)₂(dppe)₂]²⁺, obtained as its PF₆⁻ or BPh₄⁻ salt, the latter being fully characterized by single-crystal diffraction [dppe = bis(diphenylphosphino)ethane, Ph₂PCH₂CH₂PPh₂ (Capdevila, Clegg, González-Duarte, Harris, Mira, Sola & Taylor, 1992)]. More detailed examination of this reaction showed that, on some occasions, even though the experimental procedures and conditions were apparently the same, a completely different result was obtained, and the only platinum-containing product identified was [Pt₂(μ-H)(μ-S)(dppe)₂]⁺, isolated in ca 20% yield as its PF₆⁻

salt (1). The nature of this product was established by a combination of X-ray crystallography and NMR spectroscopy (Capdevila, González-Duarte, Mira, Sola & Clegg, 1992). From the room-temperature diffraction data the bridging hydride ligand could not be located and the structure included a disordered PF₆⁻ anion on a twofold rotation axis.



We subsequently prepared a fresh sample of (1) and undertook a low-temperature diffraction study with the aim of modelling the disorder better and possibly locating the hydride. We discovered that the complex undergoes a reversible phase transition on cooling below 230 K, to give an ordered structure in a unit cell of doubled volume, and were able to locate and refine the hydride position. We report here a comparison of the room-temperature and low-temperature structures, together with an account of the analogous mixed-metal PdPt complex (2), obtained in a similar way and characterized both crystallographically and spectroscopically.

2. Experimental

The synthesis of complex (1) has already been described (Capdevila, González-Duarte, Mira, Sola & Clegg, 1992). The mixed-metal complex (2) was prepared in an analogous reaction with [PdCl₂(dppe)] instead of [PtCl₂(dppe)] as one of the metal-containing starting materials. Crystals suitable for diffraction study were obtained from solution in acetonitrile. Satisfactory analyses (for C, S and H) were obtained for both complexes. Experimental details are summarized in Table 1.

Table 1. *Experimental details*

	(1) at room temperature	(1) at low temperature	(2)
Crystal data			
Chemical formula	[Pt ₂ (C ₂₆ H ₂₄ P ₂) ₂ (H)(S)](PF ₆)	[Pt ₂ (C ₂₆ H ₂₄ P ₂) ₂ (H)(S)](PF ₆)	[PdPt(C ₂₆ H ₂₄ P ₂) ₂ (H)(S)](PF ₆)
Chemical formula weight	1365.00	1365.00	1276.31
Crystal system	Monoclinic	Monoclinic	Monoclinic
Space group	<i>P</i> 2 ₁ / <i>n</i>	<i>P</i> 2 ₁ / <i>n</i>	<i>P</i> 2 ₁ / <i>n</i>
<i>a</i> (Å)	13.742 (2)	13.689 (4)	13.724 (4)
<i>b</i> (Å)	11.0580 (7)	21.857 (7)	11.097 (2)
<i>c</i> (Å)	16.7504 (14)	16.662 (5)	16.740 (4)
β (°)	96.644 (11)	95.92 (3)	96.77 (3)
<i>V</i> (Å ³)	2528.3 (4)	4958.7 (26)	2531.6 (11)
<i>Z</i>	2	4	2
<i>D_x</i> (Mg m ⁻³)	1.793	1.828	1.674
Radiation type	Mo <i>K</i> α	Mo <i>K</i> α	Mo <i>K</i> α
Wavelength (Å)	0.71073	0.71073	0.71073
No. of reflections for cell parameters	32	32	32
θ range (°)	10.16–11.82	10.20–12.25	10.19–11.80
μ (mm ⁻¹)	5.784	5.898	3.372
Temperature (K)	295 (2)	160.0 (10)	295 (2)
Crystal form	Block	Block	Block
Crystal size (mm)	0.20 × 0.18 × 0.12	0.25 × 0.25 × 0.25	0.24 × 0.20 × 0.16
Crystal colour	Yellow	Yellow	Yellow
Data collection			
Diffractometer	Stoe–Siemens diffractometer	Stoe–Siemens diffractometer	Stoe–Siemens diffractometer
Data collection method	ω/θ scans with on-line profile fitting (Clegg, 1981)	ω/θ scans with on-line profile fitting (Clegg, 1981)	ω/θ scans with on-line profile fitting (Clegg, 1981)
Absorption correction	ψ scans (SHELXTL)	ψ scans (SHELXTL)	ψ scans (SHELXTL)
<i>T</i> _{min}	0.283	0.144	0.191
<i>T</i> _{max}	0.314	0.225	0.250
No. of measured reflections	5397	10 478	5166
No. of independent reflections	4447	8708	3295
No. of observed reflections	3239	5497	2199
Criterion for observed reflections	<i>I</i> > 2 σ (<i>I</i>)	<i>I</i> > 2 σ (<i>I</i>)	<i>I</i> > 2 σ (<i>I</i>)
<i>R</i> _{int}	0.0531	0.0307	0.0429
θ _{max} (°)	25.01	25.00	22.50
Range of <i>h</i> , <i>k</i> , <i>l</i>	–16 → <i>h</i> → 16 –11 → <i>k</i> → 13 –18 → <i>l</i> → 19	–16 → <i>h</i> → 16 –3 → <i>k</i> → 25 –19 → <i>l</i> → 19	–14 → <i>h</i> → 14 –11 → <i>k</i> → 11 –18 → <i>l</i> → 18
No. of standard reflections	3	4	3
Frequency of standard reflections (min)	60	60	60
Intensity decay (%)	None	1	None
Refinement			
Refinement on	<i>F</i> ²	<i>F</i> ²	<i>F</i> ²
<i>R</i> [<i>F</i> ² > 2 σ (<i>F</i>) ²]	0.0295	0.0385	0.0366
<i>wR</i> (all data, <i>F</i> ²)	0.0683	0.0850	0.0810
<i>S</i> (all data)	1.063	1.054	1.082
No. of reflections used in refinement	4437	8679	3288
No. of parameters refined	312	599	315
H-atom treatment	See text	See text	See text
Weighting scheme	$w = 1/[\sigma^2(F_o^2) + (0.0295P)^2 + 2.8898P]$, where $P = (F_o^2 + 2F_c^2)/3$	$w = 1/[\sigma^2(F_o^2) + (0.0254P)^2 + 58.7745P]$, where $P = (F_o^2 + 2F_c^2)/3$	$w = 1/[\sigma^2(F_o^2) + (0.0409P)^2 + 2.1952P]$, where $P = (F_o^2 + 2F_c^2)/3$
(Δ/σ) _{max}	0.001	2.821	<0.001
$\Delta\rho$ _{max} (e Å ⁻³)	0.580	2.097 e Å ⁻³ ~1.1 Å from Pt	0.600
$\Delta\rho$ _{min} (e Å ⁻³)	–0.475	–1.204 e Å ⁻³ ~1.1 Å from Pt	–0.431
Source of atomic scattering factors	<i>International Tables for Crystallography</i> (1992, Vol. C, Tables 4.2.6.8 and 6.1.1.4)	<i>International Tables for Crystallography</i> (1992, Vol. C, Tables 4.2.6.8 and 6.1.1.4)	<i>International Tables for Crystallography</i> (1992, Vol. C, Tables 4.2.6.8 and 6.1.1.4)
Computer programs			
Data collection	<i>DIF4</i> (Stoe & Cie, 1988)	<i>DIF4</i> (Stoe & Cie, 1988)	<i>DIF4</i> (Stoe & Cie, 1988)
Cell refinement	<i>DIF4</i>	<i>DIF4</i>	<i>DIF4</i>
Data reduction	Local programs	Local programs	Local programs
Structure solution	<i>SHELXTL/PC</i> (Sheldrick, 1990)	<i>SHELXTL/PC</i> (Sheldrick, 1990)	<i>SHELXTL/PC</i> (Sheldrick, 1990)
Structure refinement	<i>SHELXL93</i> (Sheldrick, 1994)	<i>SHELXL93</i> (Sheldrick, 1994)	<i>SHELXL93</i> (Sheldrick, 1994)
Preparation of material for publication	<i>SHELXL93</i> and local programs	<i>SHELXL93</i> and local programs	<i>SHELXL93</i> and local programs

2.1. Room-temperature structure of (1)

The bridging hydride could not be located in difference syntheses. Its presence was deduced at this stage

from the charge balance of the complex and confirmed by NMR spectroscopy (see §3). The PF₆[–] anion was found to be disordered over a twofold rotation axis, with a well defined central position for P and a total

of eight peaks (including symmetry equivalents) in a diffuse region of significant electron density at a suitable distance from the central atom. The disorder could not be resolved into alternative orientations of an idealized octahedral PF₆⁻ group. Instead, partial F atoms were refined with anisotropic displacement parameters and with initial positions taken from the difference density map, the total occupancy of all F-atom sites being restrained to 6. The refinement leading to the results presented here was made subsequent to the preliminary communication of this structure (Capdevila, González-Duarte, Mira, Sola & Clegg, 1992) and with different software. The structure is a little more precisely described, but there are no significant changes.

H atoms other than the bridging hydride were refined with a riding model for coordinates and with $U(H) = 1.2U_{eq}(C)$; this applies to all three structures.

2.2. Low-temperature structure of (1)

Preliminary cell determination at 160 K revealed a *b* axis doubled relative to the room-temperature cell and systematic absences for $0k0$ with odd *k* indicated a change of space group from $P2/n$ to $P2_1/n$. The doubled cell volume and loss of the twofold rotation axis imply general rather than special positions for the cations and anions (assuming a simple structural relationship between the room-temperature and low-temperature phases, thus rendering unlikely the migration of anions to centres of symmetry), lifting the crystallographic symmetry imposed on both ions at room temperature. Small but significant positional and orientational changes were detected in the ions as a result of the two structure determinations and the anion was found to be ordered, with six clear fluorine positions; refinement required no restraints or constraints. The bridging hydride was also located in a difference synthesis and its position freely refined; the isotropic displacement parameter was fixed at 0.05 \AA^2 after attempted refinement gave an anomalously low value with an extremely high e.s.d. The largest Δ/σ ratio is for the *z* coordinate of the bridging H atom, which showed oscillation in alternate cycles.

Following intensity data collection, the phase transition was investigated by monitoring a reflection which has moderate intensity for the low-temperature phase but is absent (with non-integral *k* index) for the room-temperature phase, while varying the temperature with the Cryostream device employed in these experiments (Cosier & Glazer, 1986). On warming from 160 K, the reflection peak intensity declined slowly and steadily, then dropped rapidly around 230 K to give no signal significantly above background at higher temperatures. The effect was reversible, the reflection reappearing on cooling through 230 K, to be restored to its initial intensity at 160 K. Several cycles of warming and cooling through the phase transition gave no apparent deterioration of the quality of the crystal and its diffraction properties.

2.3. Room-temperature structure of (2)

Refinement was as for the room-temperature structure of (1) except for the bridging hydride and the metal atoms. The hydride was located in a difference synthesis and was refined freely with its own isotropic displacement parameter. The crystallographically unique single metal atom was treated as a composite of Pd and Pt, and the relative occupancy factors of these atoms were refined as a check on the chemical composition; the final Pt:Pd values obtained are 0.513:0.487 (7).

NMR spectra were measured with a Bruker AM-400 spectrometer, for samples in *d*₆-DMSO solution. External standards were 85% phosphoric acid and 1 *M* H₂PtCl₆/D₂O.

3. Discussion

Fractional atomic coordinates and equivalent isotropic displacement parameters for the three structures are reported in Tables 2, 4 and 6; Tables 3, 5 and 7 give selected geometric parameters.*

3.1. Room-temperature structure of (1)

A preliminary account of this has already been given (Capdevila, González-Duarte, Mira, Sola & Clegg, 1992). Further refinement on F^2 rather than F marginally improves the precision of the structure, but gives no significant difference. It was not possible to locate the bridging hydride ligand crystallographically, but the evidence from ¹H, ³¹P and ¹⁹⁵Pt NMR spectroscopy was clear and unambiguous, and the position indicated spectroscopically for this hydride is consistent with the crystallographic results and with results previously obtained both spectroscopically and crystallographically for [Pt₂(μ-H)(μ-CO)(dppe)₂](BF₄) (Minghetti, Bandini, Banditelli, Bonati, Szostak, Strouse, Knobler & Kaesz, 1983).

The identity of the other bridging ligand as S²⁻ is supported by successful structure refinement (in terms of electron density a bridging chloride would be equally acceptable, but this can be ruled out on the grounds of overall charge balance) and satisfactory elemental analysis, which included quantitative determination of sulfur and chlorine, the latter being recorded as negligible. This ligand is presumably derived from S—C bond cleavage of the original mercaptoamine ligands in the synthesis of the starting materials, but the source of the bridging hydride is obscure.

The apparent geometry of the disordered PF₆⁻ anion is essentially meaningless; the anisotropic displacement parameters of the partial F atoms are large, indicating

* Lists of atomic coordinates, anisotropic displacement parameters and structure factors have been deposited with the IUCr (Reference: FG0001). Copies may be obtained through The Managing Editor, International Union of Crystallography, 5 Abbey Square, Chester CH1 2HU, England.

Table 2. Fractional atomic coordinates and equivalent isotropic displacement parameters (\AA^2) for (1) at room temperature

	x	y	z	U_{eq}
Pt	0.22373 (2)	0.38855 (2)	0.32750 (2)	0.04434 (10)
S	1/4	0.2233 (2)	1/4	0.0669 (8)
P1	0.20559 (12)	0.5617 (2)	0.39580 (11)	0.0450 (4)
P2	0.17441 (12)	0.2916 (2)	0.43374 (11)	0.0463 (4)
C1	0.3210 (5)	0.6148 (6)	0.4480 (4)	0.050 (2)
C2	0.4025 (6)	0.6201 (8)	0.4055 (6)	0.076 (2)
C3	0.4925 (6)	0.6541 (10)	0.4434 (8)	0.097 (3)
C4	0.5034 (7)	0.6777 (9)	0.5242 (7)	0.090 (3)
C5	0.4253 (7)	0.6701 (8)	0.5676 (6)	0.082 (3)
C6	0.3326 (6)	0.6416 (7)	0.5279 (5)	0.065 (2)
C7	0.1445 (5)	0.6916 (6)	0.3454 (4)	0.051 (2)
C8	0.1884 (7)	0.8032 (8)	0.3438 (6)	0.096 (3)
C9	0.1368 (9)	0.8994 (8)	0.3060 (8)	0.125 (5)
C10	0.0436 (8)	0.8837 (9)	0.2716 (7)	0.109 (4)
C11	0.0007 (7)	0.7737 (9)	0.2713 (6)	0.096 (3)
C12	0.0503 (6)	0.6779 (9)	0.3094 (5)	0.081 (3)
C13	0.1267 (5)	0.5240 (6)	0.4738 (4)	0.056 (2)
C14	0.1621 (5)	0.4038 (6)	0.5114 (4)	0.052 (2)
C15	0.0522 (5)	0.2275 (6)	0.4105 (4)	0.053 (2)
C16	0.0015 (6)	0.2441 (8)	0.3359 (6)	0.076 (2)
C17	-0.0940 (7)	0.2035 (10)	0.3189 (7)	0.107 (4)
C18	-0.1384 (6)	0.1477 (10)	0.3769 (9)	0.106 (4)
C19	-0.0893 (8)	0.1280 (8)	0.4511 (7)	0.094 (3)
C20	0.0070 (6)	0.1706 (8)	0.4693 (6)	0.076 (2)
C21	0.2518 (5)	0.1741 (6)	0.4855 (4)	0.050 (2)
C22	0.2620 (6)	0.1671 (8)	0.5683 (5)	0.068 (2)
C23	0.3238 (7)	0.0787 (9)	0.6076 (6)	0.080 (3)
C24	0.3718 (7)	0.0002 (9)	0.5643 (7)	0.085 (3)
C25	0.3607 (6)	0.0042 (8)	0.4815 (7)	0.080 (2)
C26	0.3017 (6)	0.0917 (6)	0.4427 (5)	0.062 (2)
P3	1/4	0.4701 (4)	3/4	0.0900 (11)
F1	0.3435 (5)	0.4747 (9)	0.8131 (4)	0.141 (4)
F2	0.3204 (6)	0.4487 (14)	0.6840 (4)	0.161 (7)
F3	0.259 (2)	0.3392 (15)	0.7800 (9)	0.196 (12)
F4	0.2730 (13)	0.5935 (13)	0.7115 (9)	0.180 (9)

Table 3. Selected geometric parameters (\AA , $^\circ$) for (1) at room temperature

Pt—Pt ⁱ	2.7742 (5)	Pt—P1	2.259 (2)
Pt—S	2.294 (2)	Pt—P2	2.248 (2)
Pt—S—Pt ⁱ	74.41 (8)	S—Pt—Pt ⁱ	52.79 (4)
P1—Pt—P2	86.69 (6)	P1—Pt—Pt ⁱ	122.00 (4)
P1—Pt—S	174.56 (6)	P2—Pt—Pt ⁱ	151.13 (4)
P2—Pt—S	98.61 (6)		

Symmetry code: (i) $\frac{1}{2} - x, y, \frac{1}{2} - z$.

that the disorder is more complex and extensive than the simple model with a relatively small number of partial atoms. The disorder is largely orientational rather than displacive, since the central P atom appears to be well ordered.

Relatively high displacement parameters for some of the C atoms may indicate minor unresolved disorder in the cation (Fig. 1).

3.2. Low-temperature structure of (1)

On cooling, the *b*-axis length doubles and the space group changes from $P2_1/n$ to $P2_1/n$. The structural implications of this phase change are: (a) cations (and also anions) which are related by one unit-cell translation along **b** at room temperature are now related by a

Table 4. Fractional atomic coordinates and equivalent isotropic displacement parameters (\AA^2) for (1) at low temperature

	x	y	z	U_{eq}
Pt1	0.22971 (3)	0.19255 (2)	0.34739 (2)	0.0248 (2)
P2	0.28116 (3)	0.19439 (2)	0.19058 (2)	0.0249 (2)
S	0.2600 (2)	0.11008 (11)	0.2684 (2)	0.039 (2)
P1	0.1814 (2)	0.14328 (11)	0.4549 (2)	0.0252 (13)
P2	0.2079 (2)	0.27962 (11)	0.4158 (2)	0.0249 (13)
P3	0.2959 (2)	0.28283 (11)	0.1223 (2)	0.0243 (12)
P4	0.3296 (2)	0.14664 (11)	0.0821 (2)	0.0254 (14)
C1	0.0566 (7)	0.1132 (4)	0.4335 (7)	0.032 (5)
C2	0.0058 (9)	0.1216 (6)	0.3599 (9)	0.052 (7)
C3	-0.0906 (10)	0.1034 (7)	0.3463 (11)	0.070 (7)
C4	-0.1356 (10)	0.0760 (7)	0.4057 (14)	0.081 (7)
C5	-0.0848 (10)	0.0659 (6)	0.4794 (12)	0.066 (8)
C6	0.0122 (8)	0.0841 (5)	0.4951 (8)	0.042 (7)
C7	0.2578 (7)	0.0823 (4)	0.5050 (6)	0.027 (5)
C8	0.2705 (8)	0.0798 (5)	0.5885 (7)	0.037 (7)
C9	0.3318 (9)	0.0352 (5)	0.6256 (8)	0.045 (7)
C10	0.3805 (8)	-0.0059 (5)	0.5795 (7)	0.040 (6)
C11	0.3662 (8)	-0.0031 (5)	0.4977 (7)	0.038 (5)
C12	0.3050 (7)	0.0407 (5)	0.4582 (7)	0.033 (5)
C13	0.1710 (7)	0.1992 (5)	0.5333 (6)	0.032 (5)
C14	0.1326 (7)	0.2591 (5)	0.4965 (6)	0.029 (5)
C15	0.3235 (7)	0.3089 (5)	0.4659 (7)	0.030 (5)
C16	0.3353 (8)	0.3236 (5)	0.5462 (7)	0.039 (5)
C17	0.4269 (10)	0.3370 (6)	0.5847 (9)	0.055 (8)
C18	0.5075 (9)	0.3388 (6)	0.5415 (11)	0.059 (7)
C19	0.4954 (9)	0.3267 (6)	0.4599 (11)	0.057 (7)
C20	0.4056 (8)	0.3106 (6)	0.4222 (8)	0.047 (6)
C21	0.1441 (7)	0.3443 (4)	0.3651 (6)	0.028 (6)
C22	0.0464 (8)	0.3347 (5)	0.3328 (7)	0.036 (6)
C23	-0.0078 (9)	0.3843 (6)	0.2958 (8)	0.049 (7)
C24	0.0368 (10)	0.4398 (5)	0.2899 (8)	0.051 (8)
C25	0.1339 (11)	0.4476 (5)	0.3196 (9)	0.061 (10)
C26	0.1889 (9)	0.4007 (5)	0.3576 (7)	0.042 (7)
C27	0.3539 (7)	0.3483 (5)	0.1725 (6)	0.028 (5)
C28	0.3106 (9)	0.4065 (5)	0.1729 (7)	0.041 (7)
C29	0.3631 (10)	0.4547 (6)	0.2080 (8)	0.055 (9)
C30	0.4564 (11)	0.4479 (6)	0.2451 (8)	0.057 (10)
C31	0.5010 (9)	0.3907 (6)	0.2462 (8)	0.054 (7)
C32	0.4505 (8)	0.3419 (5)	0.2114 (7)	0.041 (6)
C33	0.1795 (7)	0.3082 (5)	0.0716 (6)	0.030 (5)
C34	0.1637 (8)	0.3189 (5)	-0.0104 (7)	0.034 (6)
C35	0.0705 (9)	0.3334 (5)	-0.0462 (8)	0.044 (7)
C36	-0.0059 (9)	0.3372 (6)	-0.0012 (10)	0.053 (6)
C37	0.0079 (9)	0.3279 (6)	0.0809 (9)	0.050 (7)
C38	0.0987 (7)	0.3122 (6)	0.1175 (7)	0.041 (5)
C39	0.3756 (7)	0.2653 (4)	0.0438 (6)	0.026 (5)
C40	0.3438 (7)	0.2043 (4)	0.0064 (6)	0.029 (4)
C41	0.4519 (7)	0.1137 (4)	0.1027 (6)	0.028 (6)
C42	0.5038 (8)	0.1208 (5)	0.1774 (7)	0.037 (6)
C43	0.5987 (9)	0.1002 (5)	0.1924 (8)	0.045 (7)
C44	0.6436 (9)	0.0711 (6)	0.1317 (8)	0.051 (6)
C45	0.5924 (9)	0.0623 (5)	0.0581 (8)	0.047 (8)
C46	0.4961 (7)	0.0834 (5)	0.0414 (7)	0.032 (6)
C47	0.2520 (7)	0.0881 (4)	0.0291 (6)	0.027 (5)
C48	0.1965 (7)	0.0490 (5)	0.0724 (7)	0.036 (5)
C49	0.1371 (9)	0.0057 (5)	0.0316 (8)	0.046 (7)
C50	0.1303 (8)	0.0008 (6)	-0.0505 (8)	0.048 (6)
C51	0.1829 (9)	0.0415 (5)	-0.0943 (7)	0.040 (7)
C52	0.2436 (8)	0.0848 (5)	-0.0544 (7)	0.037 (6)
P5	0.7410 (3)	0.2619 (2)	0.2685 (2)	0.049 (2)
F1	0.6734 (7)	0.2845 (6)	0.3351 (6)	0.100 (7)
F2	0.6442 (6)	0.2556 (4)	0.2059 (5)	0.066 (5)
F3	0.7447 (10)	0.3323 (5)	0.2443 (9)	0.142 (10)
F4	0.8372 (6)	0.2673 (5)	0.3300 (4)	0.087 (5)
F5	0.7252 (9)	0.1972 (5)	0.3023 (8)	0.142 (11)
F6	0.8030 (8)	0.2455 (11)	0.2028 (6)	0.239 (7)

2_1 screw axis and so are no longer aligned strictly collinear; (b) the crystallographic twofold rotation symmetry is no longer imposed on the cations and anions, so that the asymmetric unit of the low-temperature

Table 5. Selected geometric parameters (Å, °) for (1) at low temperature

Pt1—Pt2	2.776 (2)	Pt2—H1	1.88 (11)
Pt1—H1	1.96 (11)	Pt2—S	2.289 (3)
Pt1—S	2.295 (3)	Pt2—P3	2.263 (3)
Pt1—P1	2.248 (3)	Pt2—P4	2.246 (3)
Pt1—P2	2.254 (3)		
Pt1—H1—Pt2	93 (5)	S—Pt1—Pt2	52.64 (7)
Pt1—S—Pt2	74.54 (8)	H1—Pt2—P3	77 (3)
H1—Pt1—P1	165 (3)	H1—Pt2—P4	163 (3)
H1—Pt1—P2	79 (3)	P3—Pt2—P4	86.74 (9)
P1—Pt1—P2	86.33 (10)	H1—Pt2—S	98 (3)
H1—Pt1—S	95 (3)	P3—Pt2—S	174.76 (9)
P1—Pt1—S	99.57 (10)	P4—Pt2—S	98.46 (10)
P2—Pt1—S	173.99 (9)	H1—Pt2—Pt1	45 (3)
H1—Pt1—Pt2	43 (3)	P3—Pt2—Pt1	122.03 (7)
P1—Pt1—Pt2	151.82 (7)	P4—Pt2—Pt1	151.11 (7)
P2—Pt1—Pt2	121.58 (7)	S—Pt2—Pt1	52.82 (7)

Table 6. Fractional atomic coordinates and equivalent isotropic displacement parameters (Å²) for (2)

	x	y	z	U _{eq}
Pt	0.22353 (3)	0.38918 (4)	0.32693 (3)	0.0539 (2)
Pd	0.22353 (3)	0.38918 (4)	0.32693 (3)	0.0539 (2)
S	1/4	0.2239 (3)	1/4	0.0821 (12)
P1	0.2053 (2)	0.5619 (2)	0.39586 (14)	0.0570 (7)
P2	0.1749 (2)	0.2912 (2)	0.43317 (14)	0.0605 (7)
C1	0.3207 (6)	0.6151 (8)	0.4480 (5)	0.063 (2)
C2	0.4018 (7)	0.6207 (10)	0.4064 (7)	0.090 (3)
C3	0.4921 (8)	0.6547 (12)	0.4429 (9)	0.111 (4)
C4	0.5047 (9)	0.6773 (10)	0.5242 (9)	0.103 (4)
C5	0.4261 (10)	0.6708 (10)	0.5667 (7)	0.099 (3)
C6	0.3325 (8)	0.6408 (9)	0.5288 (7)	0.081 (3)
C7	0.1444 (7)	0.6902 (8)	0.3463 (5)	0.064 (2)
C8	0.1889 (10)	0.8031 (10)	0.3423 (8)	0.118 (4)
C9	0.1352 (14)	0.8973 (12)	0.3047 (10)	0.154 (7)
C10	0.0425 (12)	0.8833 (13)	0.2723 (9)	0.129 (5)
C11	-0.0005 (10)	0.7728 (13)	0.2722 (8)	0.121 (4)
C12	0.0515 (8)	0.6796 (10)	0.3099 (7)	0.095 (3)
C13	0.1273 (7)	0.5235 (8)	0.4739 (6)	0.071 (3)
C14	0.1632 (7)	0.4029 (7)	0.5099 (5)	0.065 (2)
C15	0.0506 (7)	0.2280 (8)	0.4094 (6)	0.066 (2)
C16	0.0014 (8)	0.2449 (10)	0.3357 (7)	0.094 (3)
C17	-0.0932 (10)	0.2046 (12)	0.3164 (9)	0.126 (5)
C18	-0.1373 (9)	0.1491 (13)	0.3727 (11)	0.123 (5)
C19	-0.0921 (10)	0.1294 (10)	0.4476 (10)	0.107 (4)
C20	0.0060 (8)	0.1700 (9)	0.4681 (7)	0.089 (3)
C21	0.2512 (6)	0.1739 (8)	0.4856 (6)	0.067 (2)
C22	0.2620 (8)	0.1657 (9)	0.5684 (6)	0.079 (3)
C23	0.3220 (10)	0.0800 (11)	0.6065 (8)	0.099 (4)
C24	0.3708 (9)	-0.0010 (12)	0.5654 (9)	0.101 (4)
C25	0.3591 (8)	0.0029 (10)	0.4837 (9)	0.100 (4)
C26	0.2998 (7)	0.0921 (8)	0.4418 (6)	0.077 (3)
P3	1/4	0.4687 (6)	3/4	0.113 (2)
F1	0.3428 (7)	0.4757 (11)	0.8123 (4)	0.167 (6)
F2	0.3205 (9)	0.4501 (18)	0.6841 (5)	0.190 (9)
F3	0.258 (2)	0.3449 (18)	0.7835 (11)	0.219 (16)
F4	0.2727 (16)	0.5916 (16)	0.7106 (11)	0.184 (11)

Table 7. Selected geometric parameters (Å, °) for (2) at low temperature

M—M ⁱ	2.7574 (11)	M—P1	2.266 (2)
M—H1	1.94 (7)	M—P2	2.252 (2)
M—S	2.295 (3)		
M—H1—M ⁱ	91 (4)	P1—M—S	174.97 (7)
M ⁱ —S—M	73.85 (10)	P2—M—S	97.96 (8)
H1—M—P2	164 (2)	H1—M—M ⁱ	45 (2)
H1—M—P1	78 (2)	P1—M—M ⁱ	122.19 (6)
P1—M—P2	86.87 (8)	P2—M—M ⁱ	150.81 (6)
H1—M—S	98 (2)	S—M—M ⁱ	53.08 (5)

Symmetry code: (i) $\frac{1}{2} - x, y, \frac{1}{2} - z$.

structure is one complete pair of ions instead of half a cation and half an anion. Comparison of the room-temperature and low-temperature structures shows that the removal of the symmetry constraint is marked by a small displacement of the cations away from their room-temperature symmetry-imposed position, the centroid of the Pt₂SH ring lying about 0.31 Å from the line 1/4, y, 1/4 in the low-temperature form; the S···H vector remains almost parallel with this line, at an angle of only 0.8°. There is a very marked reduction, by about half their values, in the equivalent isotropic displacement parameters of the cation atoms. As well as reduced dynamic freedom (thermal vibration), this may also be due to the removal of minor unresolved static disorder in the room-temperature structure. At low temperature the bridging hydride is clearly located and could be

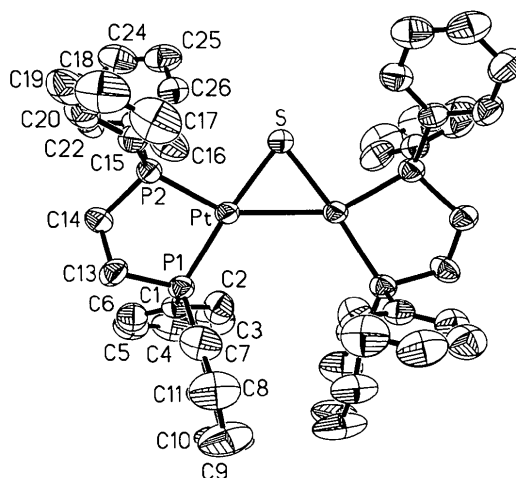


Fig. 1. The room-temperature structure of the cation of (1), with 50% probability ellipsoids and atom labelling. H atoms are omitted.

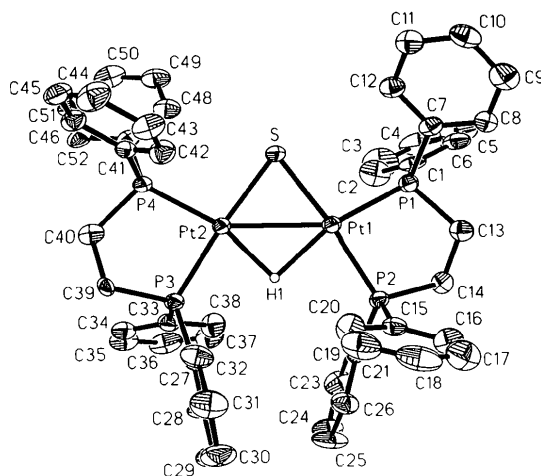


Fig. 2. The low-temperature structure of the cation of (1), with 50% probability ellipsoids and atom labelling. H atoms are omitted, except for the bridging hydride.

successfully refined with acceptable geometry, albeit with not very high precision. Apart from the hydride, the internal geometry of the cation remains essentially identical to that at room temperature (Fig. 2).

In the low-temperature phase the PF_6^- anion, not constrained by the crystallographic twofold rotation symmetry, is ordered and its refinement proceeded smoothly to give essentially octahedral geometry.

The atomic shifts involved in the interconversion of the two structures are small and the phase transition is readily characterized as a displacive order-disorder transformation. It is fully reversible on heating and

cooling through the transition temperature of *ca* 230 K. The packing of the ions in the two structures is shown in Figs. 3 and 4.

3.3. Room-temperature structure of (2)

The mixed-metal PdPt complex (2) was found to be isomorphous with the pure Pt complex (1) at room temperature, with almost identical cell parameters. Full structure determination shows that the complexes are isostructural. The major difference experimentally is that the bridging hydride can be located and refined for complex (2), with observed results which are entirely consistent with those obtained for the low-temperature structure of (1) (Fig. 5).

The two metal sites in the cation are equivalent by crystallographic symmetry. In the refinement the unique metal site was treated as a composite of Pd and Pt, which have very different X-ray scattering factors, allowing a reliable refinement of the relative site occupancy factors to give a Pt:Pd ratio of 0.513:0.487 (7), representing a small and insignificant excess of Pt over Pd. A metal site disorder of equal proportions could have two interpretations, which cannot be distinguished by purely crystallographic methods: (a) genuine heteronuclear PdPt complex ions adopting two possible orientations (Pt-Pd and Pd-Pt) at random or (b) a random mixture of equal mole proportions of homonuclear PtPt and PdPd complexes. Indeed, both types of disorder could be present together, resulting from a mixture of PtPt, PtPd and PdPd complexes in the one structure.

The question is resolved by NMR spectroscopy (^1H and ^{31}P), which also unambiguously confirms the presence of the bridging hydride ligand. The range between -2.0 and -6.0 p.p.m. of the ^1H NMR spectrum (dimethyl sulfoxide solution) shows a triplet with Pt satellites

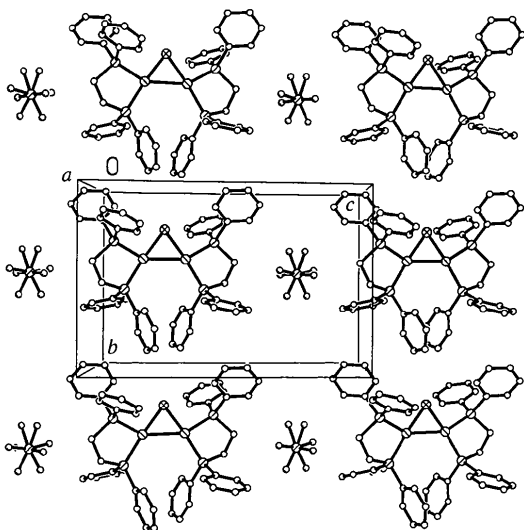


Fig. 3. A section through the crystal structure of (1) at room temperature. Only half the depth of the unit-cell contents are shown.

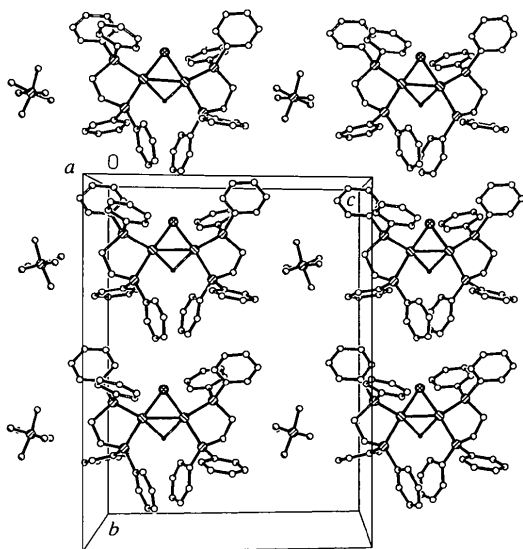


Fig. 4. A section through the crystal structure of (1) at low temperature, comparable with Fig. 3.

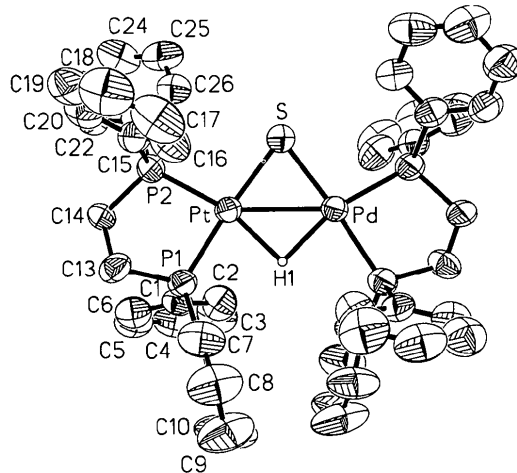


Fig. 5. The room-temperature structure of the cation of (2), with 50% probability ellipsoids and atom labelling on the assumption of a mixed-metal species, as indicated by NMR spectroscopy. H atoms are omitted, except for the bridging hydride.

due to coupling of the hydride bridge with the ¹⁹⁵Pt nucleus [$\delta = -4.57$ p.p.m., $^1J(\text{Pt}-\text{H}) = 647.3$ Hz] and with two P atoms [$^2J(\text{P}-\text{H}) = 68.3$ Hz]. The central resonance is in fact a set of three doublets, which indicates that the hydride is additionally coupled to a third P atom [$^2J(\text{P}-\text{H}) = 8.2$ Hz]. As previously reported for the PtPt analogue (1), the larger $^2J(\text{P}-\text{H})$ has been assigned to the P atoms *trans* to H and the smaller $^2J(\text{P}-\text{H})$ to those *cis* to H. However, in the heterodinuclear complex all four P atoms are non-equivalent and thus the observed pattern requires that both *trans* $^2J(\text{P}-\text{H})$ have very similar values, while those corresponding to *cis* $^2J(\text{P}-\text{H})$ are quite different, only the higher one of these being observed in the spectrum, the smaller coupling remaining unresolved. In addition, the ¹H NMR spectrum reveals that the heterodinuclear complex is somewhat contaminated (*ca* 20% for the particular solution studied) with the PtPt homodinuclear analogue as shown by a group of signals centred at -3.35 p.p.m. corresponding to the central triplet of triplets of the quintet reported for the latter complex (Capdevila, González-Duarte, Mira, Sola & Clegg, 1992); this result is consistent with the refined site occupancy factors for the two metals in the crystal structure.

The four non-equivalent phosphorus nuclei are clearly seen in the proton-decoupled ³¹P NMR spectrum, which shows two signals at δ 47.38 [P(*cis*) bonded to Pd] and 64.23 p.p.m. [P(*trans*) bonded to Pd] and two signals with ¹⁹⁵Pt satellites (1:4:1) at δ 46.37 [P(*cis*) bonded to Pt] and 60.87 p.p.m. [P(*trans*) bonded to Pt] with $^1J(\text{Pt}-\text{P})$ couplings of 2625.4 and 3550 Hz, respectively, as well as the signals corresponding to the minor presence of the PtPt analogue (at δ 43.7 and 54.9 p.p.m.). Also, the pattern of this spectrum indicates the genuine heteronuclearity of the PdPt complex, further corroborated by the fact that all the phosphorus chemical shifts differ from those observed in the PtPt analogue. By selective decoupling of the diphosphine protons (*i.e.* with the hydride still coupled), all signals except that for P(*cis*)-Pt split, displaying either P-P or P(*trans*)-H couplings. The $^2J[\text{P}(\textit{cis})-\text{H}]$ coupling is not observed because it is much smaller. Accordingly, P(*cis*)-Pd appears as a doublet [$^2J(\text{P}-\text{P}) = 32.9$ Hz], P(*trans*)-Pt as a doublet with Pt satellites [$^2J(\text{P}-\text{H}) = 67.8$ Hz] and P(*trans*)-Pd as a doublet of doublets [$^2J(\text{P}-\text{H}) = 65.7$ Hz, $^2J(\text{P}-\text{P}) = 33.8$ Hz]. These assignments require that the $^2J(\text{P}-\text{P})$ coupling constant is greater when P atoms are bonded to Pd than when they are bonded to Pt, which agrees with the fact that no measurable $^2J(\text{P}-\text{P})$ was observed in the homonuclear PtPt analogue. All coupling constants of the two spectra reported here are consistent among themselves and also with those corresponding to the PtPt complex.

The genuine heteronuclear nature of complex (2) contrasts with the results obtained for the mixed-metal PdPt product from the normal course of the synthesis,

which contains two metal ions, each chelated by a dppe ligand, bridged by two mercaptoamine ligands (Capdevila, Clegg, González-Duarte, Harris, Mira, Sola & Taylor, 1992). In that case, the evidence from crystallography, spectroscopy and chemical analysis indicated that the mixed-metal product was essentially a solid solution of the diplatinum and dipalladium complexes, with only a minor amount of the heteronuclear complex.

In all previously reported structures containing both palladium and platinum in chemically equivalent positions, the metals are disordered and crystallographic study cannot distinguish between genuine heteronuclear complexes and mixtures of homonuclear products (Clark, Ferguson, Jain & Parvez, 1985, 1986; Clark, Ferguson, Kapoor & Parvez, 1985; Suzuki, Iitaka, Kurachi, Kita, Kashiwawara, Ohba & Fujita, 1992). In some of these cases, the presence of a genuine heteronuclear complex was confirmed by NMR and mass spectrometry.

This work was supported by the UK Science and Engineering Research Council, the Comisión Interministerial de Ciencia y Tecnología, the Ministerio de Educación y Ciencia and the British Council.

References

- Capdevila, M., Clegg, W., González-Duarte, P., Harris, B., Mira, I., Sola, J. & Taylor, I. C. (1992). *J. Chem. Soc. Dalton Trans.* pp. 2817-2826.
- Capdevila, M., Clegg, W., González-Duarte, P., Jarid, A. & Lledós, A. (1996). *Inorg. Chem.* In the press.
- Capdevila, M., Clegg, W., González-Duarte, P. & Mira, I. (1992). *J. Chem. Soc. Dalton Trans.* pp. 173-181.
- Capdevila, M., González-Duarte, P., Foces-Foces, C., Hernández Cano, F. & Martínez-Ripoll, M. (1990). *J. Chem. Soc. Dalton Trans.* pp. 143-149.
- Capdevila, M., González-Duarte, P., Mira, I., Sola, J. & Clegg, W. (1992). *Polyhedron*, **11**, 3091-3093.
- Clark, H. C., Ferguson, G., Jain, V. K. & Parvez, M. (1985). *Inorg. Chem.* **24**, 1477-1482.
- Clark, H. C., Ferguson, G., Jain, V. K. & Parvez, M. (1986). *Inorg. Chem.* **25**, 3808-3811.
- Clark, H. C., Ferguson, G., Kapoor, P. N. & Parvez, M. (1985). *Inorg. Chem.* **24**, 3924-3928.
- Clegg, W. (1981). *Acta Cryst.* **A37**, 22-28.
- Cosier, J. & Glazer, A. M. (1986). *J. Appl. Cryst.* **19**, 105-107.
- Minghetti, G., Bandini, A. L., Banditelli, G., Bonati, F., Szostak, R., Strouse, C. E., Knobler, C. B. & Kesz, H. D. (1983). *Inorg. Chem.* **22**, 2332-2338.
- Sheldrick, G. M. (1990). *SHELXTL/PC Users Manual*. Siemens Analytical X-ray Instruments Inc., Madison, Wisconsin, USA.
- Sheldrick, G. M. (1994). *J. Appl. Cryst.* In preparation.
- Stoe & Cie (1988). *DIF4. Diffractometer Control Program*. Version 7.04. Stoe & Cie, Darmstadt, Germany.
- Suzuki, T., Iitaka, N., Kurachi, S., Kita, M., Kashiwawara, K., Ohba, S. & Fujita, J. (1992). *Bull. Chem. Soc. Jpn.* **65**, 1817-1824.